



Det Projection: is mathematical operation  
That is similar to the physical operation of taking  
an X-ray photograph with a collimated beam of  
radiation

---



$$P_\theta(t) = \int_{u=-\infty}^{+\infty} f_c(t_1, t_2) \Big|_{\substack{t_1 = t \cos \theta - u \sin \theta \\ t_2 = t \sin \theta + u \cos \theta}} du$$

Projection

Goal: Relate 2D F.T. of  $P_\theta$  to 1D F.T. of  $f_c$

Projection Slice Theorem

$$F_c(r_1, r_2) = \text{2-D. C.T.F.T. of } \{f_c(t_1, t_2)\}$$

$$= \int_{t_1=-\infty}^{+\infty} \int_{t_2=-\infty}^{+\infty} f_c(t_1, t_2) e^{-j r_1 t_1 - j r_2 t_2} dt_1 dt_2$$

$$F_c(r_1, r_2) = \int_{t_1=-\infty}^{+\infty} \int_{t_2=-\infty}^{+\infty} f_c(t_1, t_2) e^{-j r_1 t_1 - j r_2 t_2} dt_1 dt_2$$

$$f_c(t_1, t_2) = \frac{1}{4\pi^2} \iint F_c(r_1, r_2) e^{j r_1 t_1 + j r_2 t_2} dr_1 dr_2$$

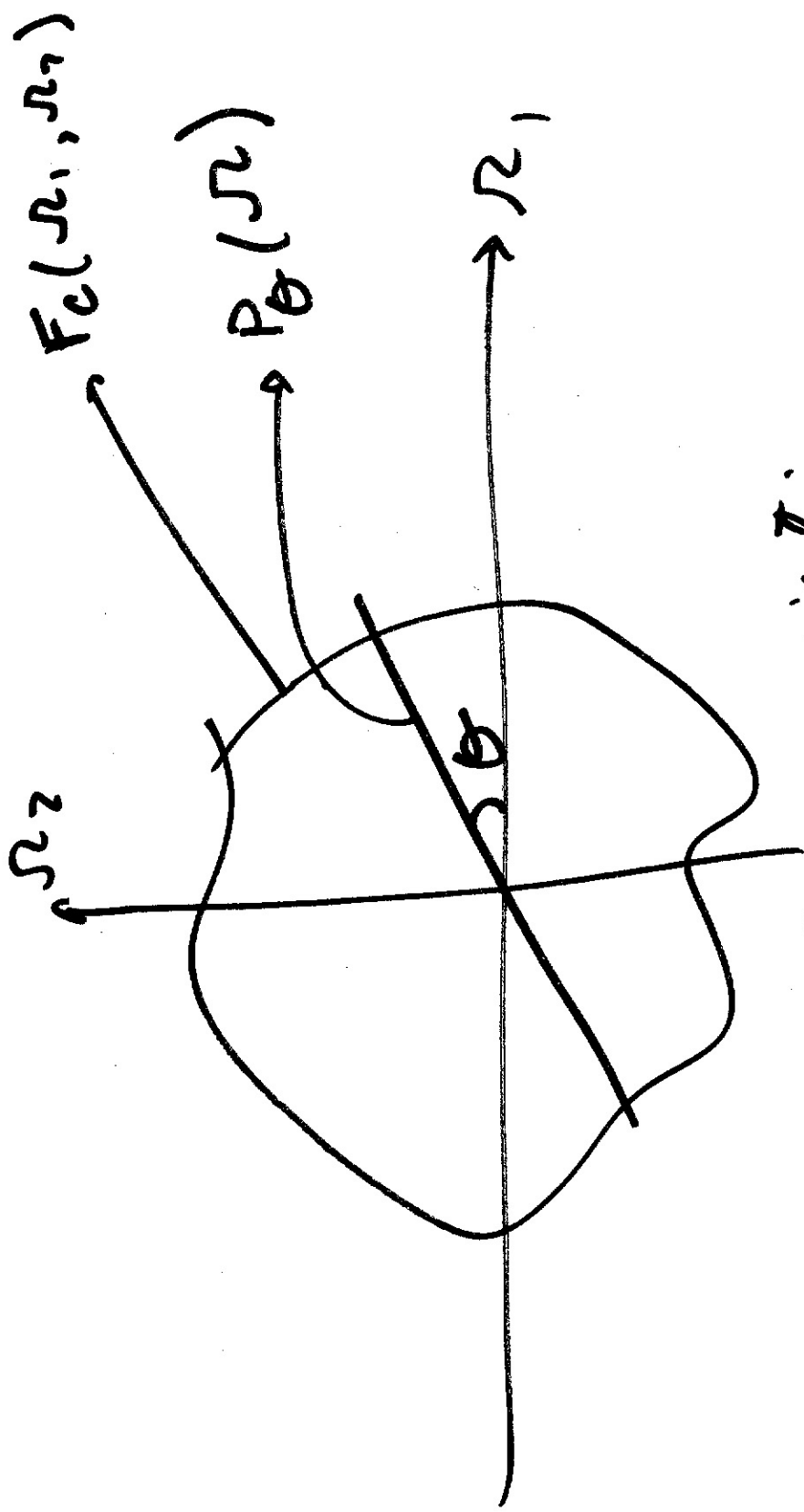
$$P_{\theta}(r) = \text{1.D. C.T.F.T. } \{P_{\theta}(t)\}$$

$$P_{\theta}(r) = \int_{t=-\rho}^{+\rho} P_{\theta}(t) e^{-jrt} dt$$

Projection Slice Theorem:

$$P_{\theta}(r) = F_c(r_1, r_2) \quad \left| \quad \begin{array}{l} r_1 = r \cos \theta \\ r_2 = r \sin \theta \end{array} \right.$$

$$P_{\theta}(r) = F_c(r \cos \theta, r \sin \theta)$$



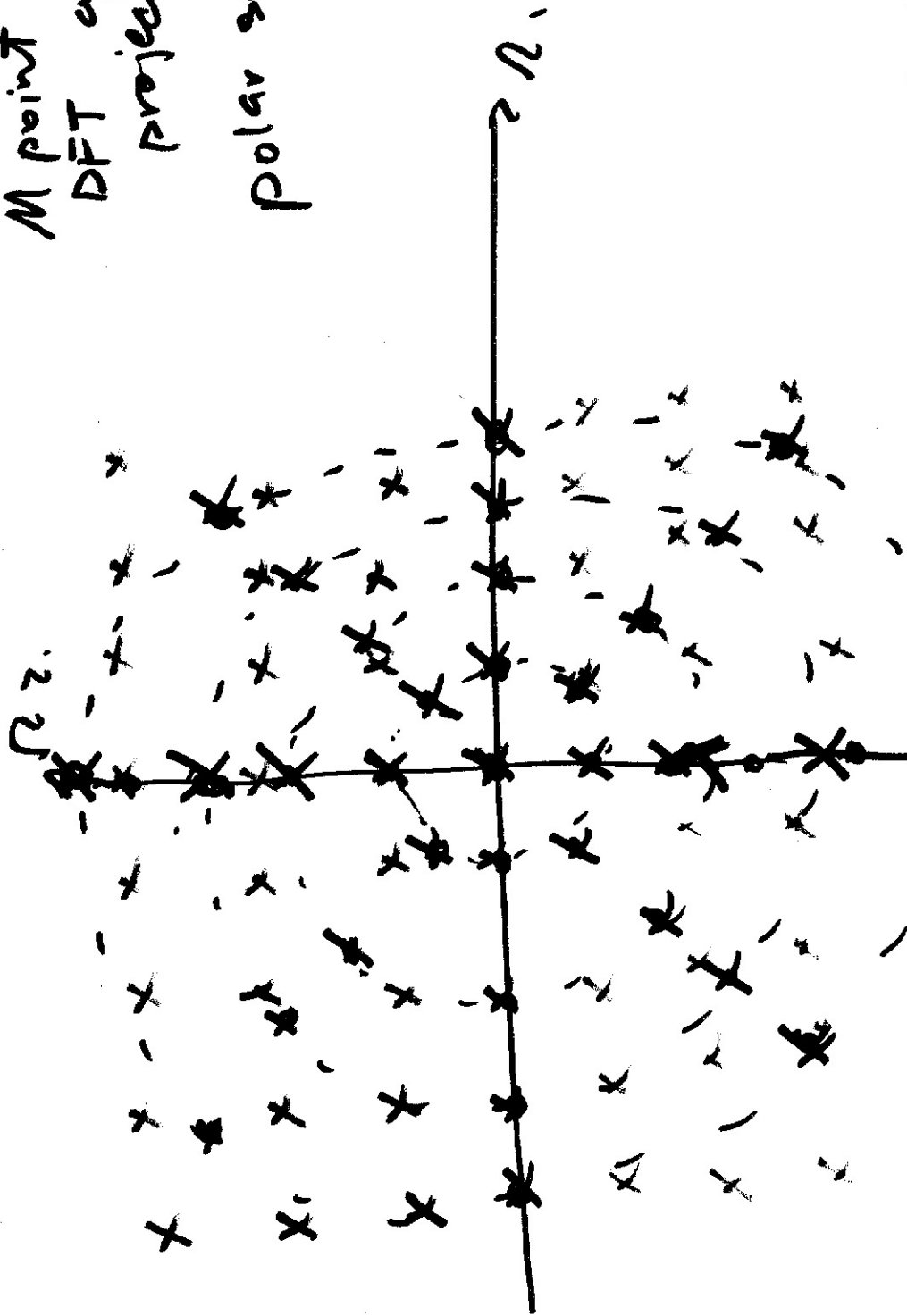
By Taking multiple projection -  
 you get 2D F.T. of the object

→ Inverse 2D. F.T

→ you get the object  $f_c(t_1, t_2)$

b

M point of  
DFT of  
projection.  
polar sampling



Polar Sampling: Every  
Fourier domain are equal.  
angle spacing samples in

To get blue cartesian samples  
from red polar sample, interpolate.

$\Rightarrow \left\{ \begin{array}{l} \text{zeroth order} \longrightarrow \text{nearest neighbor} \\ \text{1st order} \longrightarrow \text{weighted sum of} \\ \text{neighboring samples.} \end{array} \right.$

---

Concentric Squares. Distance between  
projection samples in F.D. varies a  
function of projection angle.



# Reconstruction Strategies

nearest neighbor (Zeroth order interp)

① Simple

1st order interpolation

② Radon Inversion Formula

③ Iterative technique

# Radon Inversion Formula

$$f_c(t_1, t_2) = \frac{1}{4\pi^2} \int_{-\infty}^{+\infty} \int_{-\infty}^{+\infty} F_c(r_1, r_2) e^{j r_1 t_1} e^{j r_2 t_2} e^{i r_1 d r_2} d r_1 d r_2$$

Convert To polar coordinates  $r_1, r_2 \rightarrow \omega, \theta$

$$f_c(t_1, t_2) = \frac{1}{4\pi^2} \int_0^{+\infty} \int_{-\pi}^{+\pi} F_c(\omega \cos \theta, \omega \sin \theta) e^{j \omega (t_1 \cos \theta + t_2 \sin \theta)} e^{i \omega} d\omega d\theta$$

$P_\theta(\omega)$

$$f_c(t_1, t_2) = \frac{1}{4\pi^2} \int_0^{+\infty} \int_{-\pi}^{+\pi} P_\theta(\omega) e^{j \omega (t_1 \cos \theta + t_2 \sin \theta)} e^{i \omega} d\omega d\theta$$

$$I = \int_{-\pi}^{+\pi} \left[ P_\theta(\omega) |\omega| \right] d\theta \quad \left. \vphantom{\int_{-\pi}^{+\pi}} \right\} I \quad t = t_1 \cos \theta + t_2 \sin \theta$$

Define  $G_{\theta}(\omega) = P_{\theta}(\omega) |\omega|$

$$I = \int_{-\infty}^{+\infty} \{ G_{\theta}(\omega) \} = g_{\theta}(t) \int_{-\infty}^{+\infty} \omega (t_1 \cos \theta + t_2 \sin \theta) d\omega$$

$$I = \int_{-\infty}^{+\infty} g_{\theta}(t) \Big] t = t_1 \cos \theta + t_2 \sin \theta$$

$$I = g_{\theta}(t_1 \cos \theta + t_2 \sin \theta)$$

$$f_c(t_1, t_2) = \frac{1}{4\pi^2} \int_0^{\pi} g_{\theta}(t_1 \cos \theta + t_2 \sin \theta) d\theta \quad *$$

Recall  $G_{\theta}(\omega) = P_{\theta}(\omega) / |\omega|$

$$g_{\theta}(t) = K(t) * P_{\theta}(t)$$

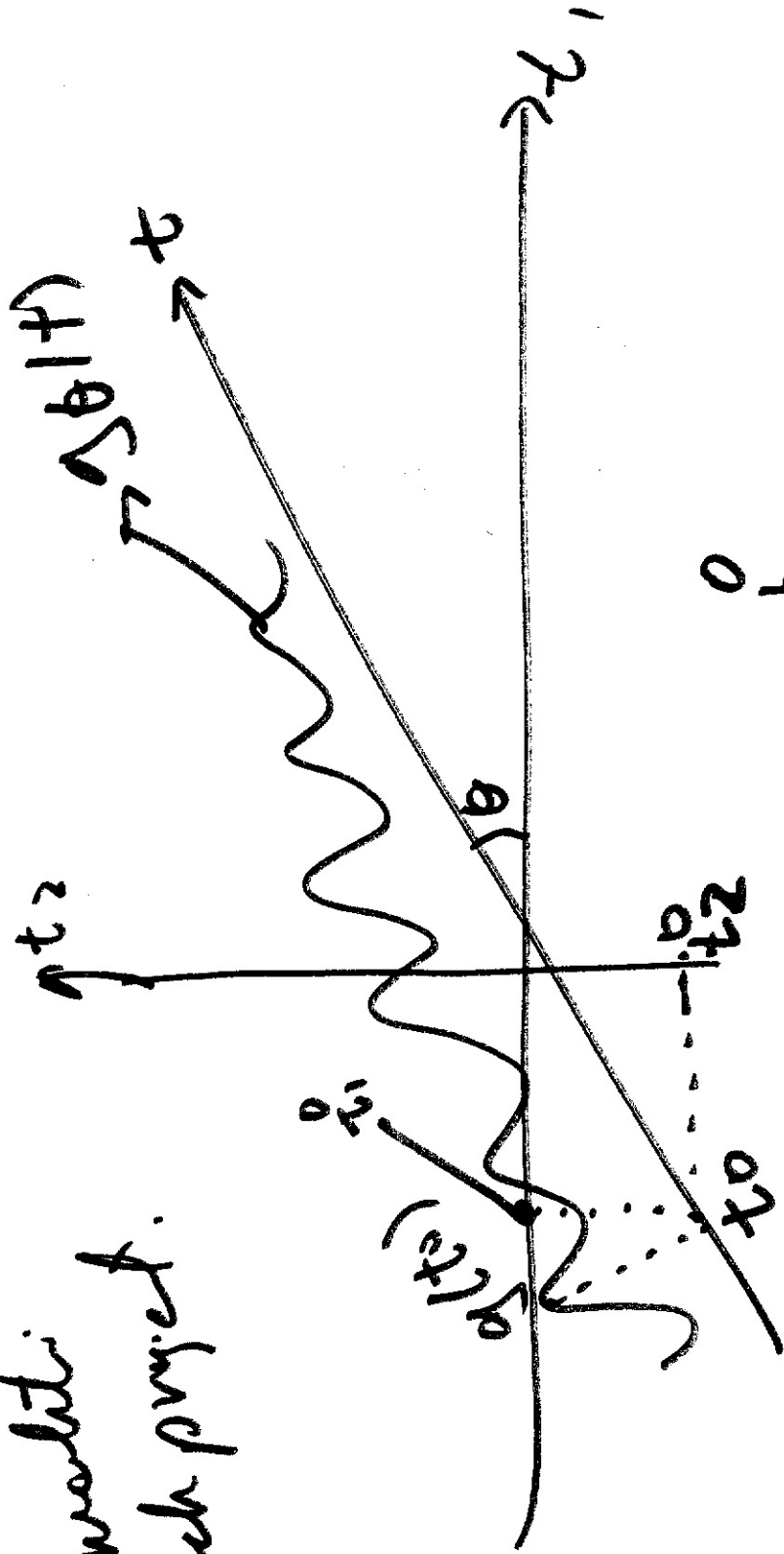
where  $K(t) = \mathcal{F}^{-1} \{ |\omega| \}$

$$g_{\theta}(t) = \frac{1}{dt} \int_{-\infty}^{+\infty} \frac{P_{\theta}(\tau)}{t-\tau} d\tau$$

Steps:

- ①  $P_{\theta}(t)$
- ② convolve with  $K(t)$  to get  $g_{\theta}(t)$
- ③ plug  $g_{\theta}(t)$  into ④

Convoluti  
Back project.



at  $t = t_0$

$t_0 \rightarrow t_1^0$   
 $t_0 \rightarrow t_2^0$

~~$$f(t_1^0, t_2^0) = g(t_0)$$~~

# Iterative Recon

$$f_c^k(t_1, t_2) = f_c^{k-1}(t_1, t_2) +$$

$$\sum_{i=1}^N \lambda_i \left[ P_{\theta_i}(t_1 \cos \theta + t_2 \sin \theta) - \right.$$

$$D_i \{ f_c^{k-1}(t_1, t_2) \}$$

determine  
convergence  
the

projection  
operation to  $k^{th}$  reconstruction  
applied to  $t_2$  vector

actual  
observed

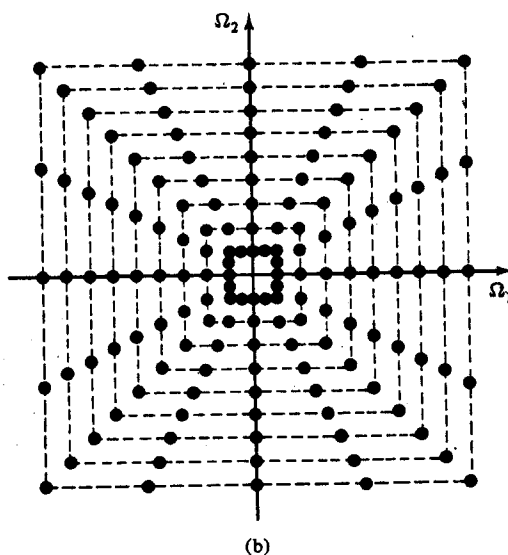
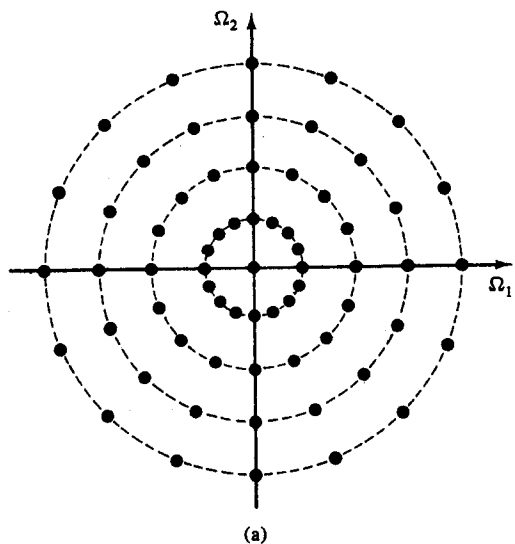


Figure 7.13 (a) Polar raster of samples in the Fourier domain, obtained by sampling all projections at the same sampling rate. (b) Concentric squares raster, obtained by varying the sampling rate with the angle of the projection. (Courtesy of Russell M. Mersereau, *Proc. IEEE*, © 1974 IEEE.)

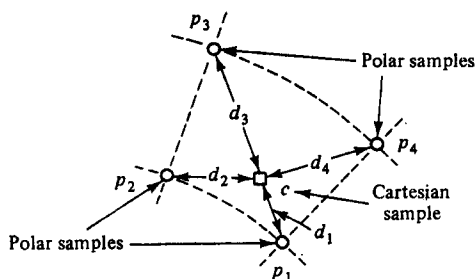
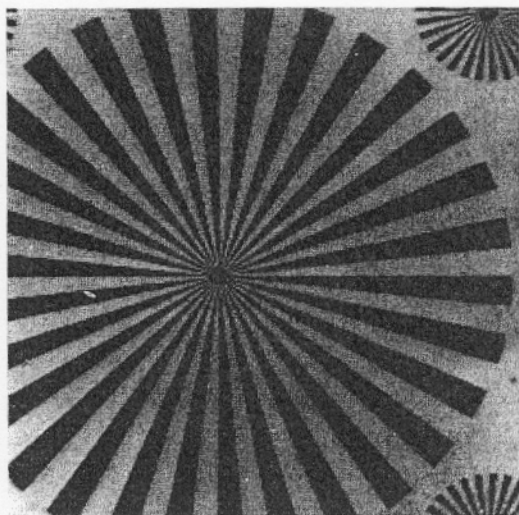
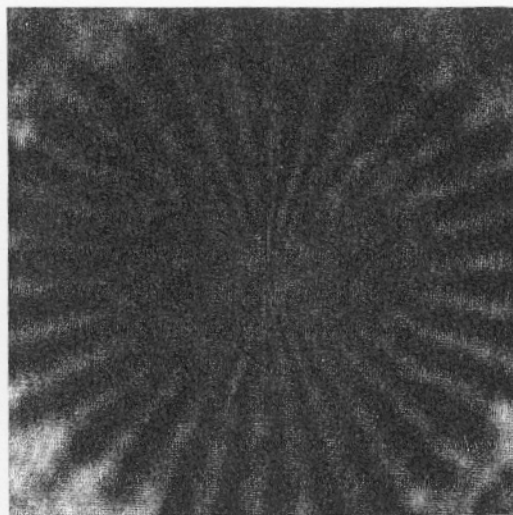


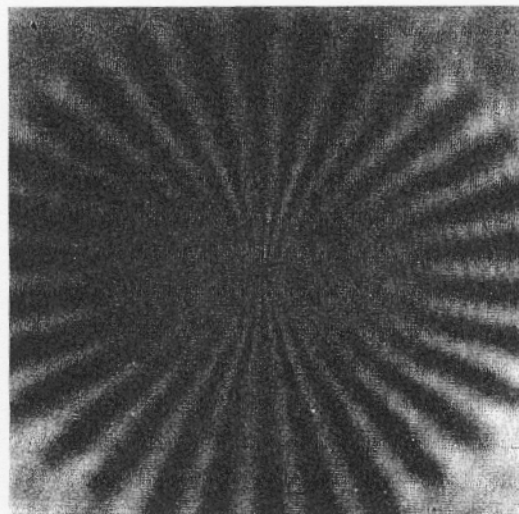
Figure 7.14 Parameters for the definition of zeroth-order and linear interpolation. (Courtesy of Russell M. Mersereau, *Proc. IEEE*, © 1974 IEEE.)



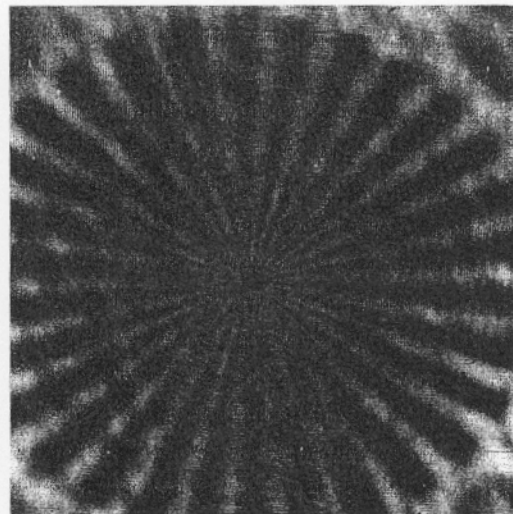
(a)



(b)



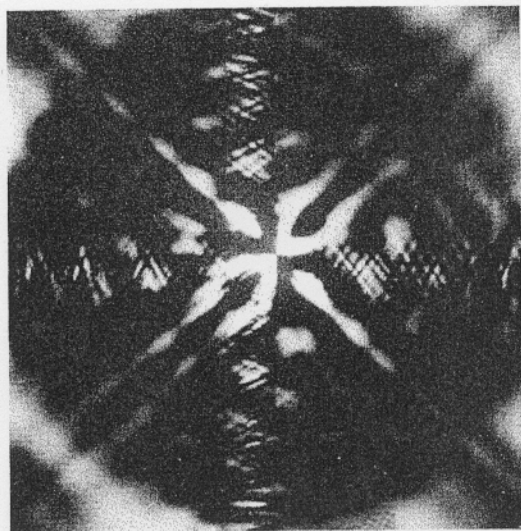
(c)



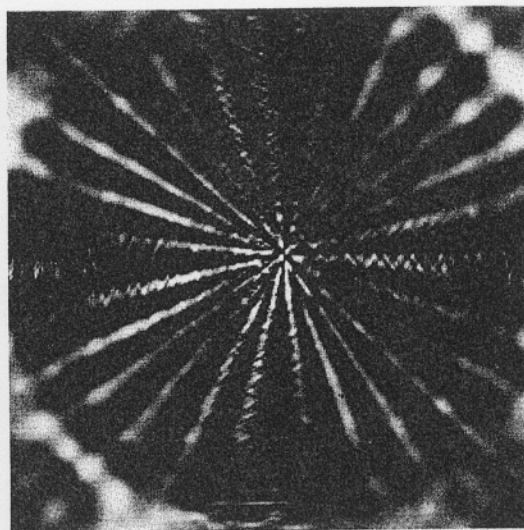
(d)

**Figure 7.15** Reconstructions of the original image shown in (a) made from 64 equiangular projections using various interpolation algorithms. (b) Zeroth-order interpolation, polar raster. (c) Linear interpolation, polar raster. (d) Linear interpolation, concentric squares raster. (Courtesy of Russell M. Mersereau, *Proc. IEEE*, © 1974 IEEE.)

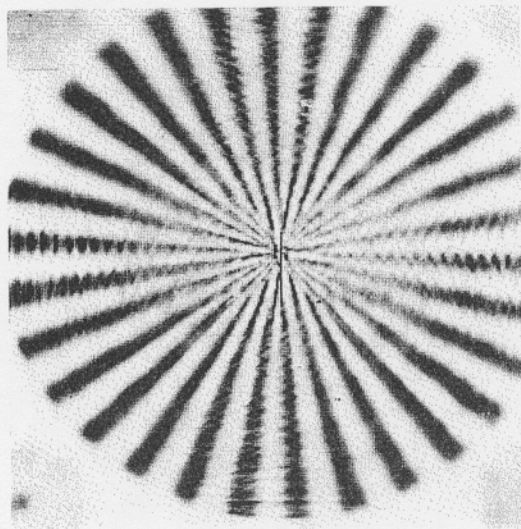




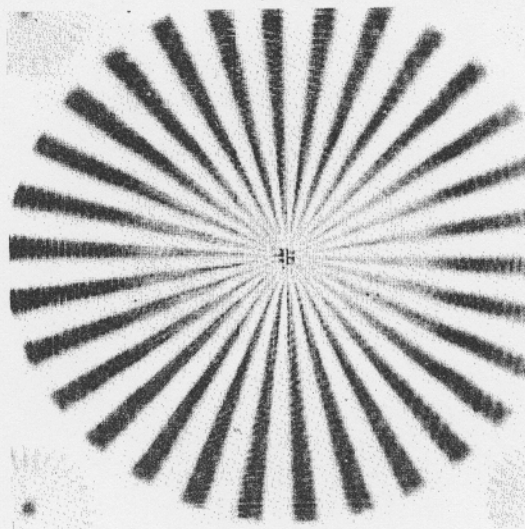
(a)



(b)



(c)



(d)

**Figure 7.16** Reconstructions made using linear interpolation from a concentric squares raster using: (a) 16 projections; (b) 32 projections; (c) 64 projections; (d) 128 projections. (Courtesy of Russell M. Mersereau, *Proc. IEEE*, © 1974 IEEE.)

filter gain increases with increasing frequency, high-frequency noise will be amplified. Thus to minimize the deterioration that can result from such noise, the filter  $k(t)$  is typically chosen to have an approximately linear response out to some cutoff frequency beyond which the response goes to zero. The exact shape of the frequency response is also governed by computational convenience [20, 21].

Some reconstructions obtained using this algorithm are shown in Figures 7.17 and 7.18. The resolution here is noticeably better than for the reconstructions

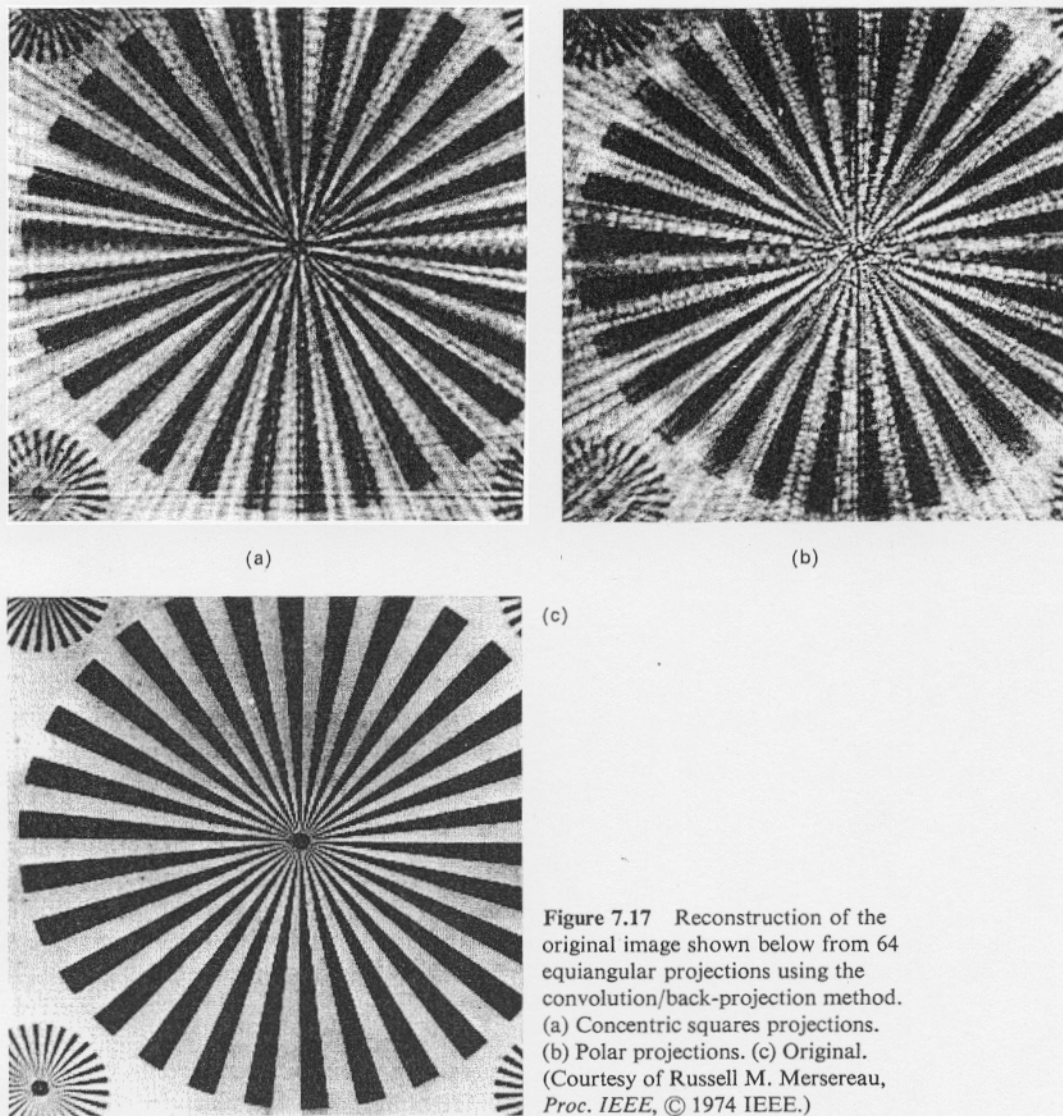
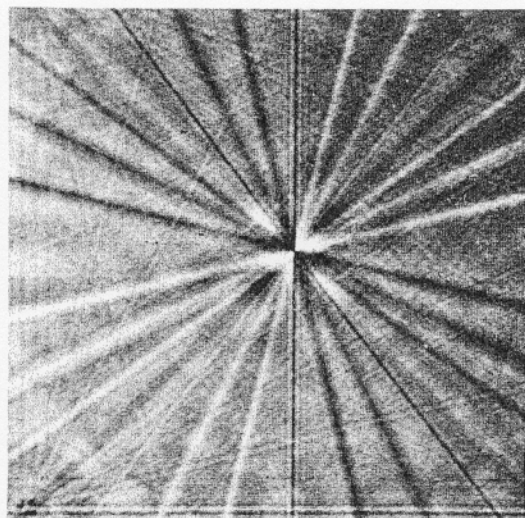
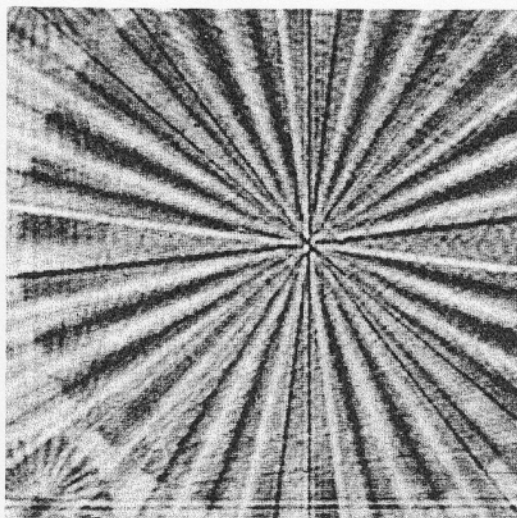


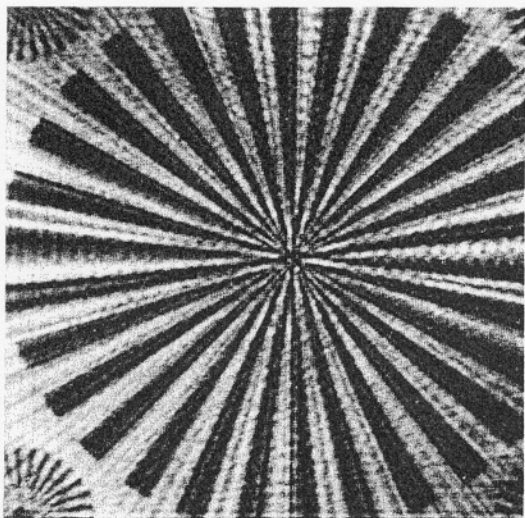
Figure 7.17 Reconstruction of the original image shown below from 64 equiangular projections using the convolution/back-projection method. (a) Concentric squares projections. (b) Polar projections. (c) Original. (Courtesy of Russell M. Mersereau, *Proc. IEEE*, © 1974 IEEE.)



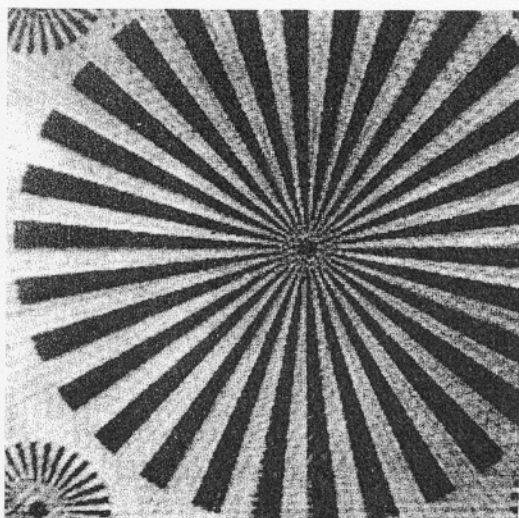
(a)



(b)



(c)



(d)

**Figure 7.18** Reconstructions made using the convolution/back-projection method applied to concentric squares projections. (a) 16 projections. (b) 32 projections. (c) 64 projections. (d) 128 projections. (Courtesy of Russell M. Mersereau, *Proc. IEEE*, © 1974 IEEE.)